JOURNAL OF Materials CHEMISTRY

Novel non-symmetric chiral twin liquid crystals possessing two identical chiral moieties at both peripheral ends: highly chirality-sensitive phases appeared between smectic and isotropic liquid phases

Isa Nishiyama,*[a] Jun Yamamoto,[a] John W. Goodby[b] and Hiroshi Yokoyama[a]

[a] *Yokoyama Nano-structured Liquid Crystal Project, JST, TRC 5-9-9 Tokodai, Tsukuba 300-2635, Japan. E-mail: isanishi@nanolc.jst.go.jp*
[b] *Department of Chemistry, The University of Hull, Hull, UK HU6 7RX*

Received 29th January 2002, Accepted 22nd March 2002
First published as an Advance Article on the web 23rd April 2002

A novel strategy for preparing non-symmetric chiral twin liquid crystals was proposed, where two identical chiral moieties were designed to be located at both peripheral ends and the non-symmetric character was introduced by the non-symmetric central connecting structure. Thus, optically active chiral non-symmetric twin homologues, [4′-(1-methylheptyloxycarbonyl)-1,1′-biphenyl-4-yl] 4‴″-[ω-[{4″-(1-methylheptyloxycarbonyl)-1″,1‴-biphenyl-4‴-yl}oxycarbonyl]alkyloxy]benzoate, were prepared, which were found to exhibit the antiferro-, ferri-, and ferroelectric phases. Furthermore, two more phases were observed between the ferroelectric and isotropic liquid phases. The lower-temperature phase was optically isotropic under the polarized light microscopy for both of the homogeneously and pseudo-homeotropically aligned thin samples, whereas the high-temperature phase showed a mosaic texture. Both of these anomalous phases were found to have a layered structure with a smaller layer spacing than the smectic phase. The stability of these phases was quite sensitive to the optical activity. With reduction of the optical purity, these phases disappeared but the Twist Grain Boundary phase was observed. A 1 : 1 mixture of (*S*,*S*)- and (*R*,*R*)-isomers just showed the smectic A phase instead of these anomalous phases.

1. Introduction

Chiral molecules generally favour formation of a helical superstructure in a liquid crystal system, which sometimes competes with the desire for molecules to pack in such a way that they fill space uniformly. Thus, introduction of chirality in liquid-crystalline systems produces a variety of frustrated phases. The experimental discovery of Twist Grain Boundary (TGB) phase[1] is a recent typical example for the appearance of the frustrated phase. The TGB phase is generated as a result of the competition between the stabilization of the smectic layered structure and the desire for the molecules to form a helical structure. Furthermore, the blue phase with a smectic layered structure, *i.e.*, smectic blue phase, has so far been obtained,[2] which has been considered to be an example that the TGB phase possesses the blue phase like superstructure.[3] These smectic blue and TGB phases have recently been investigated in detail by systematic preparation of a family of fluoro-substituted chiral compounds.[4–6] The TGB phase also shows an interesting frustrated structure if the distance between grain boundary becomes short enough to produce a "crystal of defects".[7] For example, the SmQ phase[8] has been reported to be generated as a result of the formation of a 3D crystalline network of the defect walls of the TGB phase with a local antiferroelectric structure.[7] Not only a family of the TGB phases, but also an interesting example of the effect of chirality can be seen in some dichiral mesogens,[9] where the chirality was found to play a dominant role in the appearance of the cubic superstructure.[10]

Location of the chiral moieties in the overall molecular structure seems to have a significant effect on the appearance of these chirality-induced frustrated superstructures. For example, compounds showing the SmQ phase possess an identical chiral moiety at both sides of the rigid core,[7,8,11,12] and the dichiral mesogen showing a chirality-induced cubic phase also possesses two chiral moieties with different structures at both peripheral ends of the rigid core part.[9] Recently, the introduction of chiral moieties at both ends of the central aromatic core of a molecular twin has been reported to have an important effect on the stabilization of the ferrielectric structure.[13] Since this molecular design will allow for the chiral groups to interact with each other at the interfaces between the planes of the smectic layers, stronger chiral interactions between the neighbouring smectic layers have been proposed to be obtained, and thus, the chirality-induced superstructure of the ferrielectric ordering has been stabilized. The chiral compounds reported there possess a symmetric twin structure, however, the introduction of the non-symmetric structure in twin systems has so far been reported to have a significant effect on the liquid crystal properties.[14] The non-symmetric structure is usually introduced into a twin molecular structure by connecting two different mesogenic parts. In this report, however, a novel preparative strategy for non-symmetric chiral twin liquid crystals is proposed, where a twin compound was designed in such a way that two identical chiral moieties are located at both peripheral ends, however, the non-symmetric character was generated by introducing a non-symmetric central connecting group. This molecular design allows for the molecules to possess two chiral centres at both sides of the peripheral ends, keeping strong peripheral chiral interactions, and at the same time, any special effects produced by the non-symmetric structure can be investigated.

Thus, in this study, novel non-symmetric chiral twin compounds, [4′-(1-methylheptyloxycarbonyl)-1,1′-biphenyl-4-yl] 4‴″-[ω-[{4″-(1-methylheptyloxycarbonyl)-1″,1‴-biphenyl-4‴-yl}oxycarbonyl]alkyloxy]benzoate (**I**, **II**, **III** and **IV**, see Scheme 1), were prepared and the liquid-crystalline properties were investigated. Here we report that the non-symmetric twins show anomalous phases between smectic and isotropic liquid phases, and that the stability of these phases is quite sensitive to the optical purity of the system.

DOI: 10.1039/b201061e

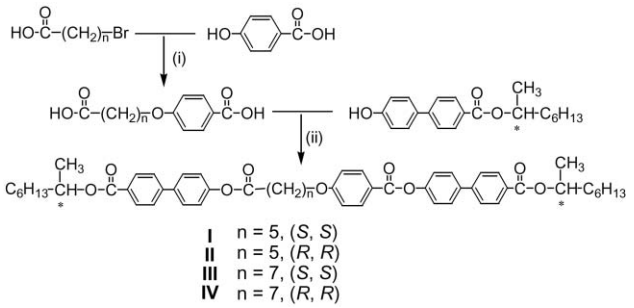

Scheme 1 The preparative route for the homologous series of non-symmetric chiral twins: (i) NaOH, EtOH–H_2O, then H^+, and (ii) DCC, DMAP, CH_2Cl_2.

2. Experimental

General preparative procedures

The non-symmetric chiral twin compounds, [4′-(1-methylheptyloxycarbonyl)-1,1′-biphenyl-4-yl]4‴′-[ω-[{4″-(1-methylheptyloxycarbonyl)-1‴,1‴′-biphenyl-4‴′-yl}oxycarbonyl]alkyloxy]benzoate (**I**, **II**, **III** and **IV**), were prepared according to Scheme 1. Final chiral twin compounds were obtained by the esterification between optically active (*S*) or (*R*)-1-methylheptyl 4-hydroxybiphenyl-4′-carboxylate and the respective 4-(ω-carboxyalkoxy)benzoic acid in the presence of dicyclohexylcarbodiimide (DCC) and *N*,*N*-dimethylaminopyridine (DMAP). 4-(ω-Carboxyalkoxy)benzoic acids were prepared by the reaction between 4-hydroxybenzoic acid and the respective ω-bromoalkanoic acids. The (*R*) and (*S*) optically active 1-methylheptyl 4-hydroxybiphenyl-4′-carboxylates were prepared according to standard procedures.[15] In the synthesis the chiral alcohols, (*S*)-octan-2-ol (Azmax. Co. Ltd., 99% ee) and (*R*)-octan-2-ol (Azmax. Co. Ltd., 99% ee), were used without further purification.

Characterisation of materials

The purification of final products was carried out using column chromatography over silica gel (70–230 mesh) (Sigma-Aldrich Co.) using a dichloromethane–hexane mixture as the eluent, followed by the recrystallization from an ethanol–ethyl acetate mixture. The purities of all of the final compounds were checked by reverse-phase and normal-phase high-performance liquid chromatography (HPLC). Reverse-phase HPLC was carried out using ZORBAX, Eclipse XDB-C8 column (diameter 4.6 mm × 150 mm) which was kept at 40 °C in an oven. Samples were dissolved in a 1 : 1 mixture of dichloromethane and methanol (or acetonitrile) and the gradient eluent system was used for elution (from water (20%) + acetonitrile (80%) to acetonitrile (100%) in 7 minutes) with a flow rate of 1.0 ml min^{-1}. Detection of products was achieved by UV irradiation (λ = 280 nm). Similarly, normal-phase HPLC was carried out using Shimadzu CLC-SIL(M) column (diameter 4.6 mm × 250 mm) which was kept at room temperature. Samples were dissolved in dichloromethane and dichloromethane was also used as an eluent. The flow rate of the eluent was 1.0 ml min^{-1}. Detection of products was achieved by UV irradiation (λ = 254 nm). Slight differences in purities obtained between reverse- and normal-phase HPLCs were observed, however, it was rather difficult to identify such a small amount of impurity. Since the obtained transition temperatures were almost identical between each (*S*,*S*)-isomer and (*R*,*R*)-isomer, which is reported later in this paper, it is expected that the impurity has little effect on the phase transition behaviour. Elemental analyses were performed using an ELEMENTAR varioEL system. The structures of the materials were elucidated by infrared (IR) spectroscopy (Shimadzu FTIR-8100A infrared spectrophotometer), proton nuclear magnetic resonance (^{1}H NMR) spectrometry (Bruker DRX500 (500 MHz), JEOL GSX400 (400 MHz) or Varian INOVA UNITY-300 (300 MHz) nuclear magnetic resonance spectrometer), and mass (MS) spectrometry (JEOL, JMS-700 using a FD/MS method). The analyses of the structures of the products and intermediates by spectroscopic methods were found to be consistent with the predicted structures.

Preparation of 4-(5-carboxypentyloxy)benzoic acid. Hydroxybenzoic acid (2.76 g, 0.020 mol) was dissolved in a mixture of ethanol (30 ml) and sodium hydroxide (2.64 g, 0.066 mol) in water (15 ml). The solution was heated and stirred while 6-bromohexanoic acid (3.90 g, 0.020 mol) was added slowly. The reaction mixture was heated under reflux for 5 hours, then a part of the solvent (25 ml) was removed by distillation. Water (100 ml) was added and the mixture was made strongly acidic with the addition of hydrochloric acid. The precipitate was isolated, dried, and recrystallized from acetic acid (42 ml), giving a colourless solid. Yield = 2.84 g, (56%). δ_H (500 MHz, DMSO, TMS) 12.25 (br, 2H, COO*H*), 7.88 (m, 2H, Ar-*H*), 7.00 (m, 2H, Ar-*H*), 4.04 (t, 2H, -CH_2-CH_2O-, ^3J = 6.5 Hz), 2.24 (t, 2H, HOCO-CH_2-CH_2-, ^3J = 7.4 Hz), 1.73, 1.57, 1.43 (m, 2H, HOCO-CH_2-CH_2-CH_2-CH_2-CH_2O-). ν/cm^{-1} (KBr) 2953–2556 (OH str.), 1696 (C=O str.), 1605 (C-C str.). *m*/*z* 252 (M^+).

Preparation of 4-(7-carboxyheptyloxy)benzoic acid. This acid was prepared from hydroxybenzoic acid (2.76 g, 0.020 mol) and 8-bromooctanoic acid (4.43 g, 0.020 mol), using the procedure given for 4-(5-carboxypentyloxy)benzoic acid, giving the product as a colourless solid. Yield = 3.56 g (64%). δ_H (400 MHz, DMSO, TMS) 12.25 (br, 2H, COO*H*), 7.87 (m, 2H, Ar-*H*), 7.00 (m, 2H, Ar-*H*), 4.03 (t, 2H, -CH_2-CH_2O-, ^3J = 6.6 Hz), 2.20 (t, 2H, HOCO-CH_2-CH_2-, ^3J = 7.3 Hz), 1.72 (m, 2H, -CH_2-CH_2-CH_2O-), 1.50–1.31 (m, 8H, HOCO-CH_2-CH_2-CH_2-CH_2-CH_2-CH_2-CH_2O-). ν/cm^{-1} (KBr) 2946–2562 (OH str.), 1690 (C=O str.), 1603 (C-C str.). *m*/*z* 280 (M^+).

Preparation of [4′-((*S*)-1-methylheptyloxycarbonyl)-1,1′-biphenyl-4-yl] 4‴′-[5-[{4″-((*S*)-1-methylheptyloxycarbonyl)-1‴,1‴′-biphenyl-4‴′-yl}oxycarbonyl]pentyloxy]benzoate (I). (*S*)-1-Methylheptyl 4-hydroxybiphenyl-4′-carboxylate (1.30 g, 4.0 mmol), 4-(5-carboxypentyloxy)benzoic acid (0.50 g, 2.0 mmol), and DMAP (0.05 g, 0.4 mmol) were added in dry dichloromethane (10 ml). DCC (1.23 g, 6.0 mmol) was then added and the resulting mixture was stirred at room temperature for one day. Precipitated materials were removed by filtration. After removal of the solvent by evaporation under reduced pressure, the product was purified by column chromatography using a dichloromethane–hexane (5 : 1) mixture as the eluent, and recrystallized from ethanol (35 ml), giving a colourless solid. Yield = 0.66 g (38%). Elemental analysis found: C% 76.0, H% 7.3, N% 0, calculated for $C_{55}H_{64}O_9$ C% 76.0, H% 7.4, N% 0. δ_H (500 MHz, $CDCl_3$, TMS) 8.17 (m, 2H, Ar-*H*), 8.10 (m, 4H, Ar-*H*), 7.66–7.63 (m, 8H, Ar-*H*), 7.31 (m, 2H, Ar-*H*), 7.19 (m, 2H, Ar-*H*), 6.99 (m, 2H, Ar-*H*), 5.17 (m, 2H, -C*$H(CH_3)$-), 4.10 (t, 2H, -CH_2-CH_2O-, ^3J = 6.3 Hz), 2.65 (t, 2H, HOCO-CH_2-CH_2-, ^3J = 7.4 Hz), 1.90–1.29 (m, 32H, aliphatic-*H*), 0.88 (two overlapping triplets, 6H, -CH_2-CH_3). ν/cm^{-1} (KBr) 2932, 2857 (C–H str.), 1755, 1709 (C=O str.), 1609 (C–C str.), 845 (1,4-disub. C-H out of plane deformation (o.o.p.d.). *m*/*z* 868 (M^+), 434, 325. HPLC purity Normal phase Si column: 100%, Reverse Phase C8 column: 99.1%.

Preparation of [4′-((*R*)-1-methylheptyloxycarbonyl)-1,1′-biphenyl-4-yl] 4‴′-[5-[{4″-((*R*)-1-methylheptyloxycarbonyl)-1‴,1‴′-biphenyl-4‴′-yl}oxycarbonyl]pentyloxy]benzoate (II). This homologue was prepared from (*R*)-1-methylheptyl 4-hydroxybiphenyl-4′-carboxylate (1.30 g, 4.0 mmol) and 4-(5-carboxypentyloxy)-benzoic acid (0.50 g, 2.0 mmol) using the procedure given for **I**, giving the product as a colourless solid. Yield = 0.88 g (51%).

Elemental analysis found: C% 76.1, H% 7.4, N% 0, calculated for $C_{55}H_{64}O_9$ C% 76.0, H% 7.4, N% 0. δ_H (400 MHz, $CDCl_3$, TMS) 8.17 (m, 2H, Ar-*H*), 8.11 (m, 4H, Ar-*H*), 7.67–7.64 (m, 8H, Ar-*H*), 7.31 (m, 2H, Ar-*H*), 7.19 (m, 2H, Ar-*H*), 6.99 (m, 2H, Ar-*H*), 5.18 (m, 2H, -C**H*(CH_3)-), 4.10 (t, 2H, -CH_2-CH_2O-, ^3J = 6.1 Hz), 2.66 (t, 2H, HOCO-CH_2-CH_2-, ^3J = 7.3 Hz), 1.91–1.29 (m, 32H, aliphatic-*H*), 0.88 (two overlapping triplets, 6H, -CH_2-CH_3). ν/cm^{-1} (KBr) 2938, 2855 (C–H str.), 1757, 1707 (C=O str.), 1609 (C–C str.), 845 (1,4-disub. C-H o.o.p.d). *m*/*z* 868 (M^+), 434. HPLC purity Normal phase Si column: 99.9%, Reverse Phase C8 column: 99.4%.

Preparation of [4′-((*S*)-1-methylheptyloxycarbonyl)-1,1′-biphenyl-4-yl] 4‴″-[7-[{4″-((*S*)-1-methylheptyloxycarbonyl)-1″,1‴-biphenyl-4‴-yl}oxycarbonyl]heptyloxy]benzoate (III). This homologue was prepared from (*S*)-1-methylheptyl 4-hydroxybiphenyl-4′-carboxylate (1.30 g, 4.0 mmol) and 4-(7-carboxyheptyloxy)-benzoic acid (0.56 g, 2.0 mmol) using the procedure given for **I**, giving the product as a colourless solid. Yield = 1.18 g (66%). Elemental analysis found: C% 76.4, H% 7.6, N% 0, calculated for $C_{57}H_{68}O_9$ C% 76.3, H% 7.6, N% 0. δ_H (300 MHz, $CDCl_3$, TMS) 8.17 (m, 2H, Ar-*H*), 8.11 (m, 4H, Ar-*H*), 7.68–7.62 (m, 8H, Ar-*H*), 7.31 (m, 2H, Ar-*H*), 7.18 (m, 2H, Ar-*H*), 6.99 (m, 2H, Ar-*H*), 5.17 (m, 2H, -C**H*(CH_3)-), 4.07 (t, 2H, -CH_2-CH_2O-, ^3J = 6.4 Hz), 2.61 (t, 2H, HOCO-CH_2-CH_2-, ^3J = 7.5 Hz), 1.85–1.29 (m, 36H, aliphatic-*H*), 0.88 (two overlapping triplets, 6H, -CH_2-CH_3). ν/cm^{-1} (KBr) 2928, 2857 (C–H str.), 1752, 1713 (C=O str.), 1609 (C–C str.), 849 (1,4-disub. C-H o.o.p.d). *m*/*z* 896 (M^+), 450. HPLC purity Normal phase Si column: 99.7%, Reverse Phase C8 column: 98.9%.

Preparation of [4′-((*R*)-1-methylheptyloxycarbonyl)-1,1′-biphenyl-4-yl] 4‴″-[7-[{4″-((*R*)-1-methylheptyloxycarbonyl)-1″,1‴-biphenyl-4‴-yl}oxycarbonyl]heptyloxy]benzoate (IV). This homologue was prepared from (*R*)-1-methylheptyl 4-hydroxybiphenyl-4′-carboxylate (1.30 g, 4.0 mmol) and 4-(7-carboxyheptyloxy)-benzoic acid (0.56 g, 2.0 mmol) using the procedure given for **I**, giving the product as a colourless solid. Yield = 1.10 g (61%). Elemental analysis found: C% 76.3, H% 7.6, N% 0, calculated for $C_{57}H_{68}O_9$ C% 76.3, H% 7.6, N% 0. δ_H (300 MHz, $CDCl_3$, TMS) 8.17 (m, 2H, Ar-*H*), 8.10 (m, 4H, Ar-*H*), 7.66–7.63 (m, 8H, Ar-*H*), 7.31 (m, 2H, Ar-*H*), 7.19 (m, 2H, Ar-*H*), 6.99 (m, 2H, Ar-*H*), 5.18 (m, 2H, -C**H*(CH_3)-), 4.07 (t, 2H, -CH_2-CH_2O-, ^3J = 6.4 Hz), 2.61 (t, 2H, HOCO-CH_2-CH_2-, ^3J = 7.5 Hz), 1.83–1.29 (m, 36H, aliphatic-*H*), 0.88 (two overlapping triplets, 6H, -CH_2-CH_3). ν/cm^{-1} (KBr) 2928, 2857 (C–H str.), 1752, 1717 (C=O str.), 1609 (C–C str.), 849 (1,4-disub. C-H o.o.p.d). *m*/*z* 896 (M^+), 450. HPLC purity Normal phase Si column: 99.9%, Reverse Phase C8 column: 100%.

Liquid-crystalline and physical properties

The initial phase assignments and corresponding transition temperatures for the final products were determined by thermal optical microscopy using an Nikon Optiphot-pol polarizing microscope equipped with a Mettler FP82 microfurnace and FP80 control unit. The heating and cooling rates were 1 °C min^{-1}. Temperatures and enthalpies of transition were investigated by differential scanning calorimetry (DSC) using a MAC Science MTC1000S calorimeter. The materials were studied at a scanning rate of 1 or 5 °C min^{-1}, after being encapsulated in aluminium pans. The X-ray scattering experiment was performed by real-time X-ray diffractometer (Bruker AXS D8 Discover). The monochromatic X-ray beam (Cu-Kαline) was generated by 1.6 kW X-ray tube and Göbel mirror optics. The 2D position sensitive detector has 1024 × 1024 pixcels in a 5 cm × 5 cm beryllium window. A sample was introduced in a thin glass capillary (diameter 1.0 mm), which was placed in a custom-made temperature stabilized holder (stability within ±0.1 °C). The X-ray diffraction measurement and the textural observation by the polarized light microscopy using a CCD camera were performed simultaneously on the sample in the glass capillary tube.

3. Results

Phase transition behaviour

Phase transition temperatures, phase sequences, and transition enthalpies for the homologous series of non-symmetric chiral twins (**I**, **II**, **III** and **IV**) are summarized in Table 1. All of the homologues studied showed the antiferro-, ferri- and ferroelectric phases, and also showed a strong tendency to exhibit pseudo-homeotropic textures in the smectic phases, when the sample was sandwiched between clean slide and cover glasses. For the pseudo-homeotropic preparation of microscope specimens of the homologues, apparent textural changes were observed at the phase transitions to and from the smectic phases. The ferrielectric phase was clearly distinguished from the antiferro- or ferroelectric phase under the polarized light microscope because the characteristic texture with constant motion as domains form, coalesce, and disappear, which had been reported for analogous monomeric materials,[16] was observed (see Fig. 1).

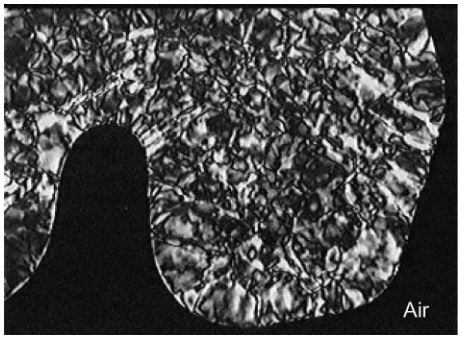

Fig. 1 The texture obtained for the ferrielectric phase of compound **I** (145 °C).

Table 1 Phase transition temperatures[a]/°C and transition enthalpies[b] /kJ mol^{-1} (in square brackets) for the non-symmetric chiral twins

	cryst		antiferro		ferri		ferro		Unidentified iso[c]		Mosaic[d]		Iso
I	●	65.9 [37.19]	●	144.4 [0.10]	●	146.7 [0.06]	●	148.8 [0.75]	●	151.0 [0.15]	●	151.5 [7.50]	●
II	●	64.1 [32.91]	●	144.5 [0.08]	●	146.6 [0.07]	●	148.7 [0.66]	●	150.7 [0.12]	●	151.2 [7.31]	●
III	●	56.4 [24.08]	●	120.4 [0.17]	●	122.0 [0.07]	●	125.7 [0.50][f]	●	128.7[e] [-][f]	●	128.7[e] [7.10]	●
IV	●	56.4 [24.87]	●	120.6 [0.15]	●	122.2 [0.05]	●	125.1 [0.62][f]	●	128.3[e] [-][f]	●	128.3[e] [7.61]	●

[a]Phase transition temperatures were determined by the polarized light microscopy on heating (scan rate = +1 °C min^{-1}) except melting temperatures which were measured by DSC (scan rate = +5 °C min^{-1}). [b]Transition enthalpies were determined by DSC measurements on heating (scan rate = +5 °C min^{-1}) for the melting, and the antiferro–ferri and ferri–ferro transitions, and on heating (scan rate = +1 °C min^{-1}) for all of the other transitions. [c]The unidentified isotropic phase looked isotropic under the polarized light microscope for thin samples. [d]The mosaic phase showed mosaic texture under the polarized light microscope. [e]The mosaic texture definitely appeared but the temperature range of the mosaic phase was quite narrow (*ca.* 0.1 °C). [f]Peaks corresponding to the ferro–unidentified isotropic and unidentified isotropic–mosaic transitions were not separated clearly, and therefore, only the total enthalpy values for the two transitions were measured.

Fig. 2 The textural change obtained for the transition from the ferroelectric phase to the unidentified isotropic phase on heating for the homogeneously aligned sample of compound **I**, where the texture of the unidentified isotropic phase appeared as lots of round shaped dark domains.

Textures for the unidentified isotropic and mosaic phases

All of the homologues showed unidentified isotropic and mosaic phases between the ferroelectric and the isotropic liquid phases. The unidentified isotropic phase appeared at a lower temperature region than the mosaic phase. The unidentified isotropic phase looked isotropic when the sample was sandwiched between two glass plates. Fig. 2 shows a textural change of compound **I** observed at the transition from the ferroelectric phase to the unidentified isotropic phase on heating for the sample which had been placed into a commercially available evaluation cell (polyimide-coated, unidirectionally buffed, 3 μm spacing, purchased from E.H.C. Co., Ltd (Japan)). The texture of the unidentified isotropic phase appeared as lots of round shaped dark domains, and on further heating, a whole region of the texture became dark which looks quite similar to an isotropic liquid phase.

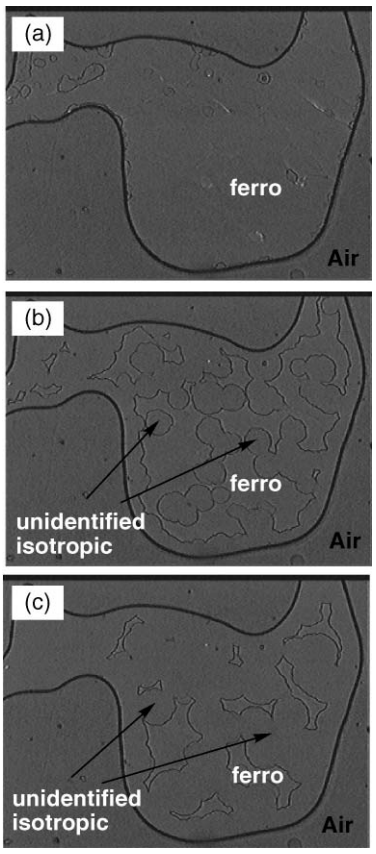

Fig. 3 The textural change obtained at the transition from the ferroelectric phase to the unidentified isotropic phase: (a) a pseudo-homeotropic texture of the ferroelectric phase, (b) the round shaped domains of the unidentified isotropic phase appeared, and (c) most regions changed into the unidentified isotropic phase.

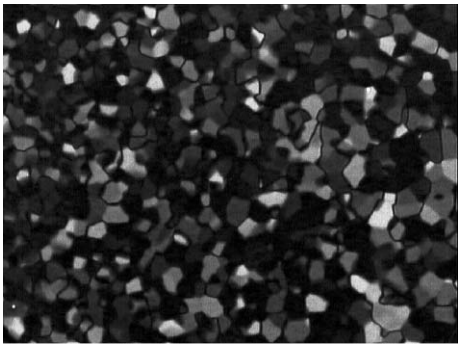

Fig. 4 The texture of the mosaic phase for compound **I** (151.3 °C).

Microscopic observation on the pseudo-homeotropically aligned sample at the ferroelectric–unidentified isotropic transition was also performed using a slightly de-crossed polarized light microscope. The textural changes of compound **I** are shown in Fig. 3. Fig. 3 (a) shows a pseudo-homeotropic texture of the ferroelectric phase. With increasing the temperature, the round shaped domains of the unidentified isotropic phase appeared (Fig. 3 (b)), and merged into each other (Fig. 3(c)).

On further heating, both the homogeneously and pseudo-homeotropically aligned samples of compound **I** showed a mosaic texture (see Fig. 4) for the mosaic phase. With further increase of temperature, the mosaic texture of the mosaic phase disappeared and the totally dark texture was again obtained under the polarized light microscopy. Compounds **II**, **III** and **IV** also showed similar textures for the unidentified isotropic and mosaic phases.

Differential scanning calorimetry thermogram

Fig. 5 shows the differential scanning calorimetry (DSC) thermogram for compound **I**, which shows small but definite peaks corresponding to the antiferro–ferri, ferri–ferro and unidentified isotropic–mosaic transitions, respectively. Transitions between mosaic and isotropic liquid phases produced a sharp DSC peak with a large transition enthalpy of 7.50 kJ mol^{-1}. Compound **II** showed a similar DSC pattern to that obtained for compound **I**, of which transition enthalpies are listed in Table 1. Fig. 6 shows the DSC thermogram for compound **III**,

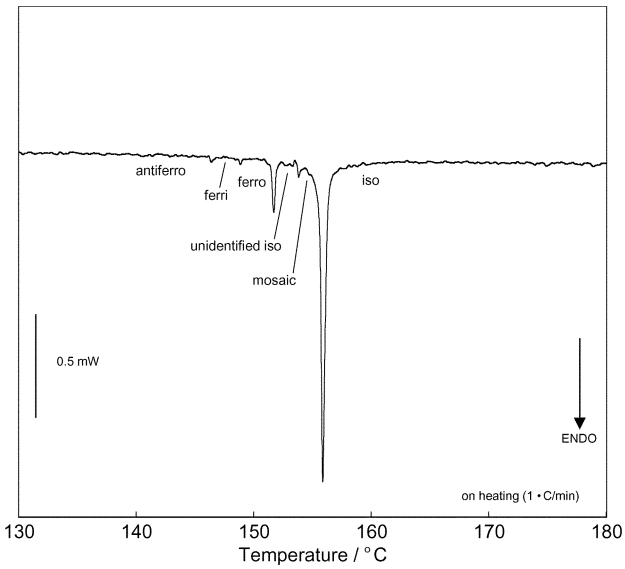

Fig. 5 The differential scanning calorimetry (DSC) thermogram for compound **I** obtained on a heating process (heating rate = 1 °C min^{-1}).

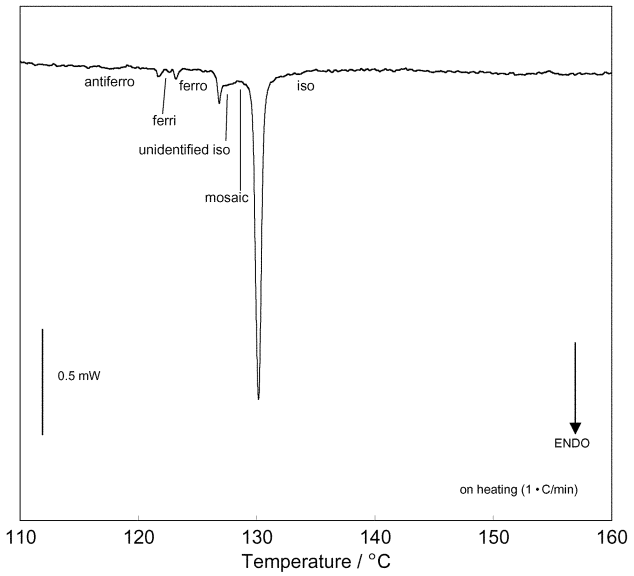

Fig. 6 The differential scanning calorimetry (DSC) thermogram for compound **III** obtained on a heating process (heating rate = 1°C min^{-1}).

which shows small but definite peaks corresponding to the antiferro–ferri and ferri–ferro transitions, respectively. However, transitions between ferro–unidentified isotropic and unidentified isotropic–mosaic this time were not separated clearly, producing a small peak with a shoulder at a higher temperature region. The transition between mosaic and isotropic liquid phases again produced a large sharp DSC peak with a transition enthalpy of 7.10 kJ mol^{-1}. Compound **IV** showed a similar DSC profile to that obtained for compound **III**, of which transition enthalpies are also listed in Table 1.

X-Ray scattering profile

Fig. 7 shows wide angle X-ray diffraction scattering patterns obtained at the antiferro, unidentified isotropic, mosaic and isotropic liquid phases of compound **II**. In the antiferroelectric phase, a sharp peak corresponding to the smectic layer spacing was observed at the small angle region, however, only diffuse scattering was observed at the wide angle region, indicating that there is no positional order within the layered structure. Similar X-ray scattering profiles were also obtained for the ferrielectric and ferroelectric phases, thus the smectic phases obtained were found to be sub-phases of the smectic C phase. Interestingly, even in the unidentified isotropic or mosaic phase, a clear peak was observed in the small angle scattering

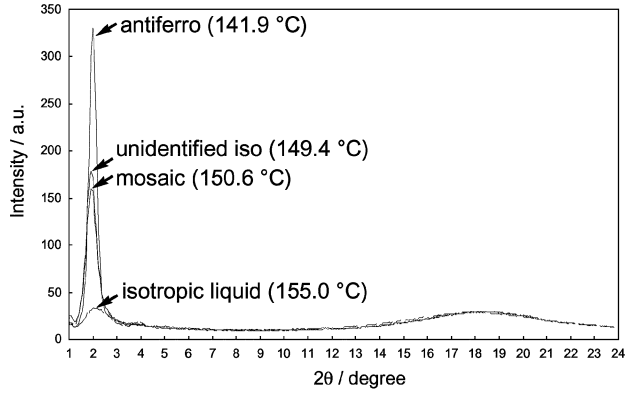

Fig. 7 Wide angle X-ray diffraction patterns obtained at the antiferro, unidentified isotropic, mosaic and isotropic liquid phases of compound **II**.

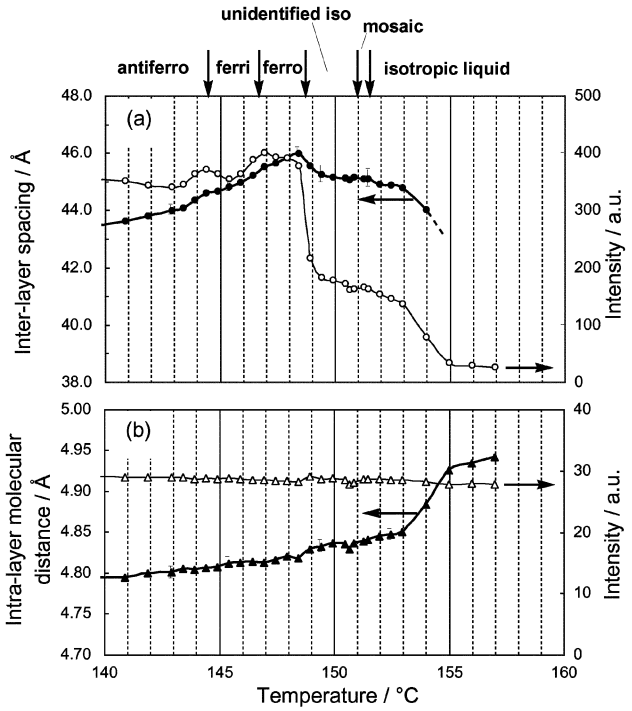

Fig. 8 (a) The inter-layer spacing and the intensity as a function of temperature for compound **II** obtained from X-ray diffraction measurements, and (b) the intra-layer molecular distance and the intensity as a function of temperature.

region, even though the peak intensities were smaller than those obtained for the smectic phases, indicating that the layered structures are more or less formed in the unidentified isotropic and mosaic phases.

Fig. 8(a) shows an inter-layer spacing obtained for compound **II** as a function of temperature. The inter-layer spacing was calculated from the peak which appeared at the low angle region of the X-ray diffraction profile. At the transition from the ferroelectric phase to unidentified isotropic phase, the intensity of the peak corresponding to the smectic layer spacing suddenly decreased, however, it remained at a certain value, indicating that the layered structure of the unidentified isotropic or mosaic phase is weaker than that of the ferroelectric phase but both of the phases have a definite layered structure. Interestingly, a layered structure was still observed *ca.* 2 °C above the mosaic–isotropic liquid transition temperature. At approximately 153 °C, the intensity of the peak corresponding to the layer spacing was again decreased suddenly, indicating the disappearance of the layered structure. The intra-layer molecular distance, *i.e.*, the distance between the molecules within each smectic layer, was estimated by the broad scattering which appeared in the wide angle region of the X-ray diffraction profile. With increasing temperature, the intra-layer molecular distance also showed a sudden change at 153 °C (Fig. 8(b)). These results strongly indicate that even in the isotropic liquid phase just above the clearing temperature, the pre-transitional molecular assemblies already occurred.

Effect of optical activity

Fig. 9 shows a phase diagram between (*R*,*R*)-isomer (compound **II**) and a 1 : 1 mixture of (*S*,*S*)- and (*R*,*R*)-isomers (**I** and **II**). The 1 : 1 mixture just showed a smectic A phase instead of showing the unidentified isotropic and mosaic phases. With increasing the optical purity, the smectic A phase was found to change into the TGB phase, which showed a typical filament texture (see Fig. 10), even though pure (*S*,*S*)- and (*R*,*R*)-isomers (**I** and **II**) themselves did not exhibit

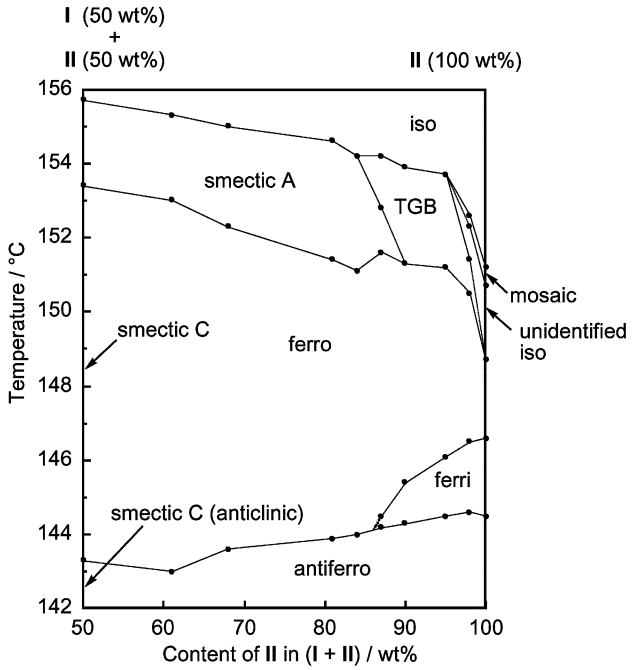

Fig. 9 A miscibility phase diagram between (*R*,*R*)-isomer (compound **II**) and the 1 : 1 mixture of (*S*,*S*)- and (*R*,*R*)-isomers (compounds **I** and **II**).

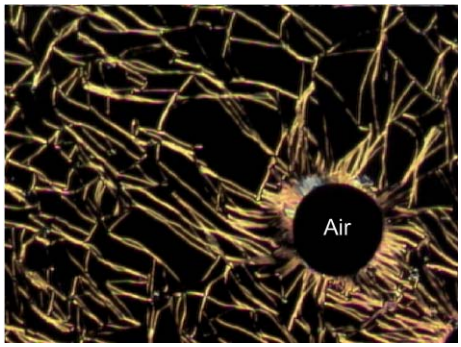

Fig. 10 A typical filament texture obtained at the transition between the smectic A and TGB phases of the mixture (87%-**II**).

the TGB phase. The clearing temperatures were found to decrease with increasing optical purity, in particular, it decreased substantially near to the pure (*R*,*R*)-isomer (**II**) in the miscibility phase diagram (Fig. 9). The stability of the ferrielectric phase also decreased when the optical purity of the system was reduced which is a similar tendency observed for the first ferrielectric compound, **MHPOBC**.[17]

The mixture containing 98% of compound **II** showed a phase sequence of mosaic–unidentified isotropic–TGB–ferro–ferri–antiferro. Fig. 11 shows the textural change of the mixture (98%-II) observed for the homogeneously aligned sample in a cell (3 μm thickness). Fig. 11(a) shows a broken fan-shaped texture for the ferroelectric phase which was changed into the *Grandjean* texture of the TGB phase with increasing temperature. Fig. 11(b) shows a phase transition from the TGB phase to the unidentified isotropic phase, where the TGB phase showed a *Grandjean* texture (blue and green in colour) and the unidentified isotropic phase appeared as lots of dark round-shaped domains. On further heating, the completely dark texture of the unidentified isotropic phase changed into mosaic texture (see Fig. 11(c)), as a result of the appearance of the mosaic phase.

Smectic layer spacings for two of the mixtures between compounds **I** and **II** were obtained from X-ray diffraction

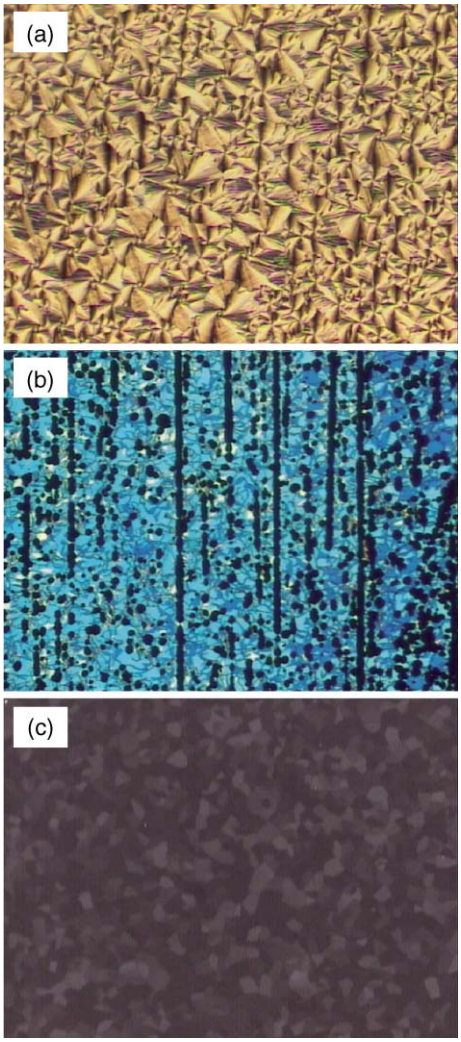

Fig. 11 The textural change of the homogeneously aligned sample of the mixture (98%-**II**): (a) the broken fan texture of the ferroelectric phase, (b) at the transition between the TGB phase (the *Grandjean* texture) and the unidentified isotropic phase (the dark domains), and (c) the mosaic texture of the mosaic phase.

measurements, and are shown in Fig. 12 as a function of reduced temperature ($T - Tc$; Tc = the clearing point). One mixture (**II** (84%) + **I** (16%)) showed a ferro–smectic A phase sequence, and the other mixture (**II** (95%) + **I** (5%)) showed a

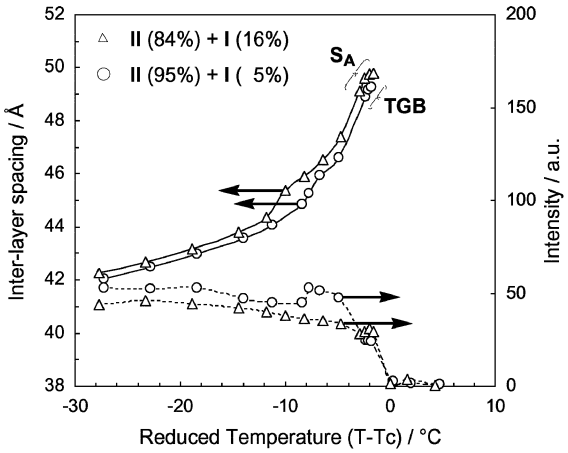

Fig. 12 The inter-layer spacing and the intensity as a function of temperature obtained from X-ray diffraction measurements: (△) the mixture with 84% of compound **II**, (○) the mixture with 95% of compound **II**.

ferro–TGB transition due to the increase of the optical activity. The layer spacing of the TGB phase is similar to that of the smectic A phase, indicating that the obtained TGB phase has a local structure of the smectic A type molecular ordering.

4. Discussion

Two anomalous phases, *i.e.*, unidentified isotropic and mosaic phases, produced by the non-symmetric chiral twin homologues were found to be thermodynamically stable phases because DSC peaks were obtained associated with respective transitions. Since these phases turned into the TGB phase when the optical purity of the system was reduced, the unidentified isotropic and mosaic phases are considered to possess more strongly twisted molecular assemblies than the TGB structure. Thus, one possible assignment of these phases is the smectic blue phase. This assumption is consistent with the X-ray diffraction scattering results which clearly showed that the unidentified isotropic and mosaic phases possess a layered structure. Interestingly, the layer spacing obtained for the unidentified isotropic and mosaic phases (*ca.* 45 Å, see Fig. 8) was found to be smaller than that obtained for the TGB phase (*ca.* 49 Å, see Fig. 12), whereas the TGB phase showed a similar smectic layer spacing to the smectic A phase of the 1 : 1 mixture of the (*S*,*S*)- and (*R*,*R*)-isomers. These results indicate that the TGB phase possesses a local smectic structure similar to the original smectic A phase but the unidentified isotropic and mosaic phases have a different local smectic structure. If molecules align in such a way that they form a more disordered or locally twisted structure in the smectic layer in the unidentified isotropic and mosaic phases, then the shorter smectic layer spacing can be obtained. The unidentified isotropic and mosaic phases are considered to produce a highly twisted structure so that the locally twisted molecular assembly could be one possible reason for the shortening of the layer spacing. The gradual decrease of the layer spacing during the temperature range of the smectic blue phase has so far been reported,[5,6] however, compound **II** studied here showed almost a constant layer spacing value in the region of the unidentified isotropic and mosaic phases.

So far the smectic blue phases have only been obtained between the isotropic liquid phase and the TGB_A or TGB_C phase.[5] The non-symmetric chiral twin homologues studied here however exhibited the unidentified isotropic and mosaic phases between the ferroelectric smectic C phase and the isotropic liquid phase. If the unidentified isotropic and mosaic phases are kinds of the smectic blue phases, the homologues are the first examples showing the smectic blue phase without the TGB phases. When the optical purity of the (*R*,*R*)-isomer was decreased, a phase sequence of "TGB–unidentified isotropic–mosaic–isotropic liquid" was obtained, thus the (*S*,*S*)- and (*R*,*R*)-isomers themselves are considered to favour a strong helical structure which makes molecules twist in not only one direction as in the TGB phases but also in the two radial directions forming the smectic blue structures.

The mosaic texture obtained for the mosaic phase is somewhat similar to the SmQ phase,[12] however, no indication of the appearance of the SmQ phase was obtained in the X-ray diffraction scattering. Moreover, the SmQ phase has been reported to be a strongly twisted TGB phase with a local antiferroelectric structure and always appears between the antiferroelectric and isotropic liquid phases, so that the phase sequence obtained here, *i.e.*, antiferro–ferri–ferro–unidentified isotropic–mosaic–isotropic liquid, is not consistent with the emergence of the SmQ phase.

The smectic blue–isotropic liquid transition has so far produced rather a broad DSC peak,[4–6] where the smectic blue phase just below the isotropic liquid was assigned to be a BPIII-type fog phase. It should be noted however that the homologues showed a sharp DSC peak at the mosaic–isotropic liquid transition. Thus, the mosaic phase may not be a BPIII-type phase. Also the enthalpy corresponding to the mosaic–isotropic liquid transition of the chiral twins, *i.e.*, a range from 7.1 to 7.6 kJ mol^{-1}, is larger than the reported values[4] corresponding to the transition between the BPIII-type fog phase and the isotropic liquid phase (0.8 to 2.9 kJ mol^{-1}),[4] also suggesting that the mosaic phase has a different character from the BPIII-type fog phase. The SmQ phase has also been reported to show smaller enthalpies (0.2 to 0.7 kJ mol^{-1}) at the SmQ–isotropic liquid transition,[12] which again suggests that the mosaic is not the SmQ phase. It should be noted that the unidentified isotropic and mosaic phases were quite viscous under the shearing of the samples which had been placed between two glass plates. This result also indicates that the unidentified isotropic phase has, to some extent, an organized structure. The X-ray diffraction measurement showed a clear peak in the small angle region so that the layered structure was proposed for the unidentified isotropic and mosaic phases. However, a cubic or columnar type structure cannot be totally ruled out for these new phases at this stage of work. Detailed studies on the viscoelastic properties are now in progress for investigating the structures of these phases.

5. Conclusions

Optically active non-symmetric twin homologues possessing two identical chiral moieties at both peripheral ends exhibited an "antiferro–ferri–ferro–unidentified isotropic–mosaic–Iso" phase sequence. The unidentified isotropic and mosaic phases were found to possess a layered structure, however, the layer spacing of these phases was smaller than that of the smectic phase. These phases were quite sensitive to the optical purity of the compound. With a reduction in the optical purity, the unidentified isotropic and mosaic phases changed into the TGB phase, and eventually, the smectic A was obtained for the 1 : 1 mixture of the (*S*,*S*)- and (*R*,*R*)-isomers, suggesting that the unidentified isotropic and mosaic phases possess more strongly twisted molecular assemblies than the TGB structure. Thus, the unidentified isotropic and mosaic phases are considered to have a smectic blue phase like molecular ordering.

References

1 J. W. Goodby, M. A. Waugh, S. M. Stein, E. Chin, R. Pindak and J. S. Patel, *J. Am. Chem. Soc.*, 1989, **111**, 8119; J. W. Goodby, M. A. Waugh, S. M. Stein, E. Chin, R. Pindak and J. S. Patel, *Nature*, 1989, **337**, 449.
2 E. Demikhov and H. Stegmeyer, *Liq. Cryst.*, 1991, **10**, 869.
3 H.-S. Kitzwerow, in *Chirality in Liquid Crystals*, eds. H.-S. Kitzerow and C. Bahr, Springer-Verlag, New York, 2001, p. 346.
4 M.-H. Li, V. Laux, H.-T. Nguyen, G. Sigaud, P. Barois and N. Iseart, *Liq. Cryst.*, 1997, **23**, 389.
5 E. Grelet, B. Pansu and H.-T. Nguyen, *Liq. Cryst.*, 2001, **28**, 1121.
6 C. D. Cruz, E. Grelet, J. C. Rouillon, J. P. Marcerou, G. Sigaud, B. Pansu and H.-T. Nguyen, *Liq. Cryst.*, 2001, **28**, 1415.
7 A. M. Levelut, E. Hallouin, D. Bennemann, G. Heppke and D. Lötzsch, *J. Phys. II*, 1997, **7**, 981.
8 A. M. Levelut, C. Germain, P. Keller, L. Liebert and J. Billard, *J. Phys.*, 1983, **44**, 623.
9 A. Yoshizawa, J. Umezawa, N. Ise, R. Sato, Y. Soeda, T. Kusumoto, K. Sato, T. Hiyama, Y. Takanishi and H. Takezoe, *Jpn. J. Appl. Phys.*, 1998, **37**, L942; T. Kusumoto, K. Sato, M. Katoh, H. Matsutani, A. Yoshizawa, N. Ise, J. Umezawa, Y. Takanishi, H. Takezoe and T. Hiyama, *Mol. Cryst. Liq. Cryst.*, 1999, **330**, 227.
10 Y. Takanishi, H. Takezoe, A. Yoshizawa, T. Kusumoto and T. Hiyama, *Mol. Cryst. Liq. Cryst.*, 2000, **347**, 257.
11 A. M. Levelut, D. Bennemann, G. Heppke and D. Lötzsch, *Mol. Cryst. Liq. Cryst.*, 1997, **299**, 433.
12 D. Bennemann, G. Heppke, A. M. Levelut and D. Lötzsch, *Mol. Cryst. Liq. Cryst.*, 1995, **260**, 351.

13 I. Nishiyama, J. Yamamoto, J. W. Goodby and H. Yokoyama, *J. Mater. Chem.*, 2001, **11**, 2690.
14 For example, C. T. Imrie and G. R. Luckhurst, in *Handbook of Liquid Crystals*, eds. D. Demus, J. W. Goodby, G. W. Gray, H.-W. Spiess and V. Vill, Wiley-VCH, Weinheim, 1998, vol. 2B, p. 801; V. Faye, H.-T. Nguyen, V. Laux and N. Isaert, *Ferroelectrics*, 1996, **179**, 9; A. E. Blatch, I. D. Fletcher and G. R. Luckhurst, *J. Mater. Chem.*, 1997, **7**, 9.
15 E. Chin and J. W. Goodby, *Mol. Cryst. Liq. Cryst.*, 1986, **141**, 311.
16 J. W. Goodby, J. S. Patel and E. Chin, *J. Mater. Chem.*, 1992, **2**, 197.
17 M. Fukui, H. Orihara, Y. Yamada, N. Yamamoto and Y. Ishibashi, *Jpn. J. Appl. Phys.*, 1989, **28**, L849; A. D. L. Chandani, E. Gorecka, Y. Ouchi, H. Takezoe and A. Fukuda, *Jpn. J. Appl. Phys.*, 1989, **28**, L1265.